PROCEEDINGS OF SCIENCE

Scattering Observables from Few-Body Densities and Application in Light Nuclei

Alexander Long,[a,*] **Harald W. Grießhammer,**[a] **Andreas Nogga**[b] **and Xiang-Xiang Sun**[b]

[a] *The George Washington University*
Washington DC USA

[b] *Name of Andreas' institution here*

E-mail: alexlong@gwu.edu, hgrie@gwu.edu, a.nogga@fz-juelich.de, x.sun@fz-juelich.de

The dynamics of scattering on light nuclei is well understood, but its calculation is numerically difficult using standard methods. Fortunately, using recent developments, the relevant quantities can be factored into a product of the n-body transition density amplitude (TDA) and the interaction kernel of a chosen probe. These TDAs depend only on the target, and not the probe; they are calculated once and stored. The kernels depend on only the probe and not the target, moreover they can be reused for different targets. The calculation of the transition densities becomes numerically difficult for $n \geq 4$, but we discuss a solution through use of a renormalization group transformation. This technique allows for extending the density transition method to ^{4}He and ^{6}Li. Throughout this work, Compton scattering is used as test bed, since its kernel is well-developed, but extension to pion-photoproduction and other reactions are discussed as well.

The 11th International Workshop on Chiral Dynamics (CD2024)
26-30 August 2024
Ruhr University Bochum, Germany

*Speaker

© Copyright owned by the author(s) under the terms of the Creative Commons Attribution-NonCommercial-NoDerivatives 4.0 International License (CC BY-NC-ND 4.0) All rights for text and data mining, AI training, and similar technologies for commercial purposes, are reserved. ISSN 1824-8039 . Published by SISSA Medialab.

1. Introduction

This can be 10 pages. Anything is red is a question or something that needs to be fixed.

I am a little unclear on how much discussion of effective field theories, and general intro information is needed here.

The transition density method was pioneered by Grießhammer *et al.* [1]. We seek to analyze an incoming probe, interacting with an A body target. This probe therefore, may interact with $1, 2, ..., A$ nucleons. The n nucleons it interacts with we call *active* and $A - n$ it does not we call *spectators*. The mathematical description of these two parts are completely separate; the n active nucleons contribute to the n-body kernel, and spectator nucleons contribute to the density. The n-body kernel represents the interaction in the idealized case where the probe interacts with only the n-body system. For example, the one-body kernel of Compton scattering contains exactly the same contributions as Compton scattering off a Nucleon. The complete separation of these two parts means if one has access to a different kernels and b different TDAs, then ab different results can be produced. Figure 1 provides an example for the case $A = 3$.

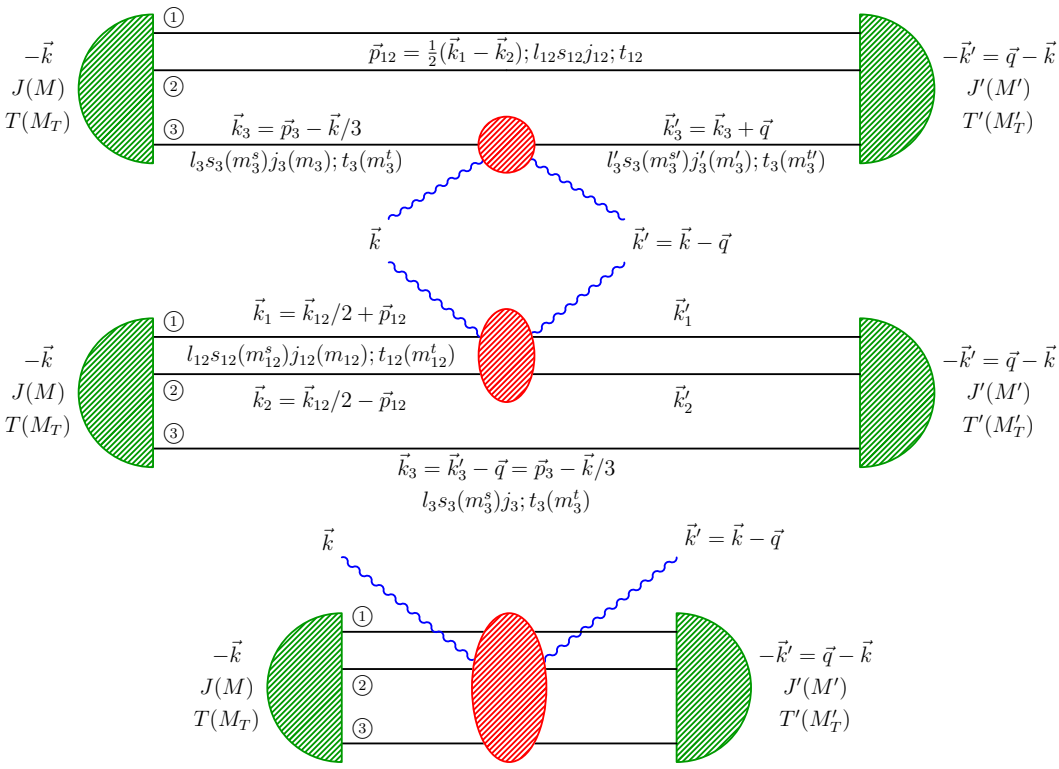

Figure 1: Kinematics in the center of mass frame and quantum numbers for an $A = 3$ system in the case of Compton scattering. Generalization to other reactions only changes the kind of ingoing/outgoing probe. Top: one-body processes $\hat{O}_3$, center: two-body processes $\hat{O}_2$, bottom: three-body processes $\hat{O}_3$. Green represents the densities, and red represents the kernels. From Grießhammer *et al.*[1]

For scattering off an A-body nucleus, the total scattering amplitude is given by

$$\begin{aligned} A_M^{M'}(\vec{k},\vec{q}) = &\binom{A}{1}\langle M'|\,\hat{O}_1(\vec{k},\vec{q})\,|M\rangle + \binom{A}{2}\langle M'|\,\hat{O}_2(\vec{k},\vec{q})\,|M\rangle \\ &+\binom{A}{3}\langle M'|\,\hat{O}_3(\vec{k},\vec{q})\,|M\rangle + \binom{A}{4}\langle M'|\,\hat{O}_4(\vec{k},\vec{q})\,|M\rangle \\ &+\ldots+\binom{A}{A}\langle M'|\,\hat{O}_A(\vec{k},\vec{q})\,|M\rangle\,, \end{aligned} \tag{1}$$

where $\hat{O}_i$ is the i-body kernel, M, M' is the spin of the target nucleus, and there are $\binom{A}{i}$ ways for a probe to hit i nucleons. Fortunately, χEFT provides a hierarchy of scales which predicts decreasing contributions for higher order terms for probe energies greater than $\sim$ 40MeV. *your note says you want a reference here, what do you mean?* Therefore, the 3-body contribution and higher is negligible at this order, and we simply use

$$A_M^{M'}(\vec{k},\vec{q}) = \binom{A}{1}\langle M'|\,\hat{O}_3(\vec{k},\vec{q})\,|M\rangle + \binom{A}{2}\langle M'|\,\hat{O}_2(\vec{k},\vec{q})\,|M\rangle$$

In practice this is enough for accuracy on roughly the 5% level.

2. Kernels and Densities

I do not think this is specific to the $A = 3$ system, but it is taken DIRECTLY from my thesis proposal. The one-body and two-body kernel must be considered separately. Their form is completely different, and they require a one- and two-body density respectively. We now write the wave function in the three body system as a partial-wave decomposition of Jacobi momenta p_i and the relevant quantum numbers α. The wave function in momentum space is given by

$$\psi_\alpha(p_{12},\, p_3) = \langle p_{12}p_3\alpha|M\rangle\,. \tag{2}$$

The nucleus being described has total angular momentum J and spin-projection M. The momenta are $\vec{p}_{12} = \frac{1}{2}\left(\vec{k}_1 - \vec{k}_2\right)$ where $\vec{p}_3 = \vec{k} + \frac{1}{3}\vec{k}_3$, and $p_{12} = |\vec{p}_{12}|$ and $p_1 = |\vec{p}_1|$. Here $\vec{k}_i$ are the individual nucleon momenta, and $\vec{k}$ is the probe momentum in the CM frame. The quantity α represents all the quantum numbers of the nucleons inside the nucleus [1]

$$|\alpha\rangle = |[(l_{12}s_{12})\,j_{12}\,(l_3s_3)\,j_3]\,JM,\,(t_{12}t_3)\,TM_T\rangle\,, \tag{3}$$

Here s, l and j are the spin, orbital and total angular momentum respectively. The quantum number s_3 simply represent the spin of nucleon 3, whereas s_{12} represents the total spin of the 1-2 subsystem; the quantities l_{12} and j_{12} combine the 1-2 subsystem similarly. Furthermore, s_{12} and l_{12} combine to j_{12} and likewise for l_3, s_3 and j_3. Finally j_{12} and j_3 combine to the total nucleus spin J. The same combinations are done for t_{12}, t_3 and T, with isospin projection M_T. Here t_3 and t_{12} are the isospin of the nucleon labeled 3 and the 1-2 subsystem respectively, T is the isospin of the entire nucleus and M_T is defined as the difference between the number of protons and neutrons divided by 2. We now seek to describe the scattering amplitudes.

We restrict ourselves to elastic processes, which simplifies the following discussion by requiring that the probe does not alter the charge of the nucleons *you have a note saying you want me to add "not of the nucleus", I am confused by this* . For the one body density, the *one-body kernel* of the probe interaction with nucleon 3 is O_3. Leaving nucleons 1 and 2 as spectators [1],

$$\left\langle \vec{k}_3' \middle| \left\langle s_3 m_3^{s\prime} \middle| \left\langle t_3 m_3^{t\prime} \middle| \hat{O}_3(\vec{k},\vec{q}) \middle| t_3 m_3^t \right\rangle \middle| s_3 m_3^s \right\rangle \middle| \vec{k}_3 \right\rangle \equiv \delta_{m_3^{t\prime} m_3^t} \delta^{(3)}\left(\vec{k}_3' - \vec{k}_3 - \vec{q}\right) O_3\left(m_3^{s\prime} m_3^s m_3^t; \vec{k}_3; \vec{k}, \vec{q}\right), \tag{4}$$

where m_t and m_t' are the isospin of the active nucleon before and after the interaction (recall $m_t = \pm\frac{1}{2}$ is the proton/neutron). Symbolically, the matrix element $\hat{O}_3$ is:

$$\begin{aligned}\left\langle M' \middle| \hat{O}_1(\vec{k},\vec{q}) \middle| M \right\rangle = \sum_{\alpha\alpha'} \int & \mathrm{d}p_{12} p_{12}^2 \, \mathrm{d}p_3 p_3^2 \, \mathrm{d}p_{12}' p_{12}'^2 \, \mathrm{d}p_3' p_3'^2 \psi_{\alpha'}^\dagger \left(p_{12}' p_3'\right) \psi_\alpha \left(p_{12} p_3\right) \\ & \times \left\langle p_{12}' p_3' \left[\left(l_{12}' s_{12}'\right) j_{12}' \left(l_3' s_3\right) j_3'\right] J' M' \left(t_{12}' t_3\right) T' M_T \middle| \hat{O}_1(\vec{k},\vec{q}) \right. \\ & \left. \middle| p_{12} p_3 \left[\left(l_{12} s_{12}\right) j_{12} \left(l_3 s_3\right) j_3\right] J M \left(t_{12} t_3\right) T M_T \right\rangle .\end{aligned} \tag{5}$$

The central result is that up to relativistic corrections, this can be written as:

$$\left\langle M' \middle| \hat{O}_1(\vec{k},\vec{q}) \middle| M \right\rangle = \sum_{\substack{m_3^{s\prime} m_3^s \\ m_3^t}} \hat{O}_1\left(m_3^{s\prime} m_3^s, m_3^t; \vec{k}, \vec{q}\right) \rho_{m_3^{s\prime} m_3^s}^{m_3^t M_T, M' M}(\vec{k},\vec{q}) . \tag{6}$$

Here ρ, is the *one-body transition density amplitude* for the nucleus which was discussed previously and can truly be interpreted as the probability amplitude that nucleon m_3^t absorbs momentum $\vec{q}$, changes its spin projection from m_s^3 to $m_s^{3'}$ and changes the spin-projection of the nucleus from M to M'. Its operator form is

$$\rho_{m_3' m_3^s}^{m_3^t M_T, M' M}(\vec{k},\vec{q}) = \left\langle M' \middle| s_3 m_3^{s\prime}, t_3 m_3^t \right\rangle \mathrm{e}^{\mathrm{i}\frac{2}{3}\vec{q}\cdot\vec{r}_3} \left\langle s_3 m_3^s, t_3 m_3^t \middle| M \right\rangle . \tag{7}$$

The two body case works similarly, and results in

$$\left\langle M' \middle| \hat{O}_2 \middle| M \right\rangle = \sum_{\alpha_{11}', \alpha_{12}} \int \mathrm{d}p_{12} \, p_{12}^2 \, \mathrm{d}p_{12}' \, p_{12}'^2 \, O_2^{\alpha_{12}' \alpha_{12}}\left(p_{12}', p_{12}\right) \rho_{\alpha_{12}' \alpha_{12}}^{M_T, M' M}\left(p_{12}', p_{12}; \vec{q}\right) . \tag{8}$$

This is the two-body equivalent to (6). There is an expression analogous to (5) but, it is non-trivial and for our purposes non-enlightening. This two-body density $\rho_{\alpha_{12}' \alpha_{12}}^{M_T, M' M}$ is of course completely distinct from the one-body density. However, just like the one-body case it can also be interpreted as a probability density. It depends on the incoming and outgoing quantum numbers α_{12} and α_{12}' of the 1-2 system, and also on the relative momenta of the two nucleons which are integrated over. As a result, the total file size for the two nucleon densities are on the order of a few GB per energy and angle, whereas those of the one nucleon densities are on the order of a few KB. Importantly, ρ can be computed directly from a nuclear potential, such as the chiral SMS potential without reference to the kernel $\hat{O}_1$ or $\hat{O}_2$ [2]. *Maybe this is too much detail. Later if we run out of space we can cut the intro discussion and just use the definitions of the one/two body operators.*

3. SRG Transform

Previous work using the TDA formalism has analyzed ^{3}He and ^{4}He, but to extend this to ^{6}Li involves many-body interactions which are much more complicated, and computationally expensive [1, 3]. To make the calculation of a TDA feasible for $A = 6$, a *similarity renormalization group* (SRG) transformation is employed [4]. When using nuclear potentials, we approximate the potential as zero beyond a certain cutoff Λ, and consequently neglect contributions above this cutoff in our calculations In general, a nuclear potential, such as the chiral SMS potential does not fall off rapidly at high momenta. As a result we would have to extend the cutoff much further than we would like, which in turn increases computational cost. The SRG transform is a unitary transformation that shifts the relevant physics into the low-momentum region, thereby lowering minimum effective cutoff. This, in turn, significantly improves the convergence rate of calculations for $A = 6$. The SRG transformation can be thought of as a local averaging or smoothing of the potential, resulting in decreased resolution has the SRG is applied. In the under-evolved, high resolution figure 2a one

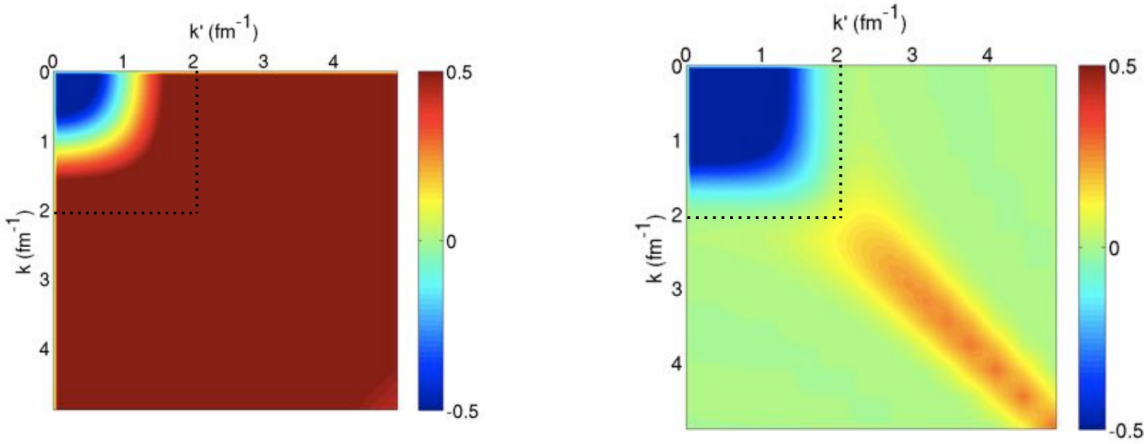

(a) High Resolution (before much SRG is applied)

(b) Low Resolution (evolved)

Figure 2: Nuclear potentials $V(k, k')$. Figures from Kai Hebeler: "Chiral Effective Field Theory and Nuclear Forces: overview and applications" presentation at TALENT school at MITP 2022, and modified with permission from Furnstahl *et al.*[16].

can see the potential does not go to zero rapidly whereas once the transformation is applied in figure 2b it does. As a result a cutoff can be made at *I like calling it k here, not* Λ $k, k' = 2\text{fm}^{-1}$ without losing much accuracy. In the example above, the under-evolved potential had to be considered up to $k, k' = 5\text{fm}^{-1}$, this means an efficiency gain proportional to the areas of each, for a factor of $(5/2)^2 = 6.25$.

However, this creates another problem: the SRG transform creates a change in the physical

meaning of the free variables. In fact, any unitary transform also transforms the coordinates.

$$\begin{aligned}\langle p'|\, V\, |p\rangle &= \langle p'|\, \mathbb{1} V \mathbb{1}\, |p\rangle \\ &= \langle p'|\, U^{\dagger} U V U^{\dagger} U\, |p\rangle \\ &= \left(\langle p'|\, U^{\dagger}\right)\, \left(U V U^{\dagger}\right)\, \left(U\, |p\rangle\right) \\ &= \langle \widetilde{p}\,'|\, V_{eff}\, |\widetilde{p}\rangle = V_{eff}(\widetilde{p}, \widetilde{p}\,')\end{aligned} \tag{9}$$

So referring to the free variables in an SRG-transformed potential as "momenta" is, to some extent, abuse of notation. They do not represent physical states *you have a note here "variables are states?" what do you mean by this?* in the sense that $\widetilde{p}$ = 50MeV does not correspond to a state of 50 MeV an experimentalist can prepare. The Lagrangians that generate the Feynman diagrams in the kernel, however, depend on physical momenta, and therefore we cannot directly use an SRG evolved potential in the non-SRG evolved kernel. To solve this, previous work with SRG transformations has transformed the Lagrangians - and therefore the kernels - into the SRG evolved space as well. However, in the context of the density formalism this would mean adding SRG dependence into the kernel, thereby breaking kernel-density independence. Additionally, the SRG transformation can take many different forms; we wish to allow for these developments without having to re-write the kernel code [16] *I'm citing the review here* . Therefore we have chosen to apply an inverse transformation to the densities [17].

The SRG evolution has parameters that must be fine-tuned, but this allows for uncertainty estimation. In particular an expansion in the harmonic oscillator basis is used. When expanded to infinite order, this basis forms a complete set. However, we truncate this expansion, including only N_{tot} terms. Additionally, the harmonic oscillator basis has a characteristic width, denoted by ω_H, and finally, the parameter Λ_{SRG} represents the resolution of the potential, as seen in figure 2. All of these parameters affect the resulting cross-section. We note that uncertainty decreases monotonically with increasing N_{tot}, since at $N_{\text{tot}} = \infty$ the associated uncertainty goes to zero. Applying a stronger SRG evolution to the potential results in larger induced many-body forces; however, the overall effect of this uncertainty is small. Fortunately, when the TDA is calculated we also gain access to the binding energy of the simulated system. From this, we can estimate optimal values for ω_H and Λ_{SRG} by comparing the experimental binding energy to simulated binding energy. This work was initiated with the highest nucleon-number system for which TDAs can calculate without an SRG transformation, namely ^{4}He. In this way we gained confidence in our approach for ^{4}He before moving to the more complex ^{6}Li.

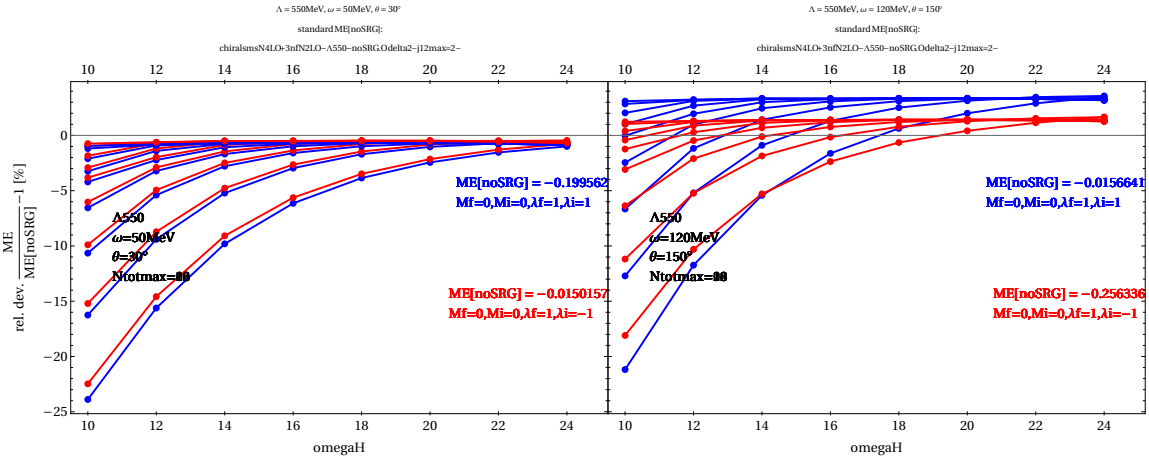

Figure 3: A convergence plot for ^{4}He Compton scattering . *This is a stand-in, need convergence plots from you.*

In figure 3, we see the effectiveness of the results in the ^{4}He case. The figure 3 shows the combined effect of both of these truncations; we expect the deviation to decrease as N increases, and importantly for our analysis, this shows what value of N is required. With this completed we have now moved to ^{6}Li. This is of much interest experimentally since this target is stable solid at room temperature, it is therefore easy to conduct an experiment on, even to high precision due to its relatively large cross section.

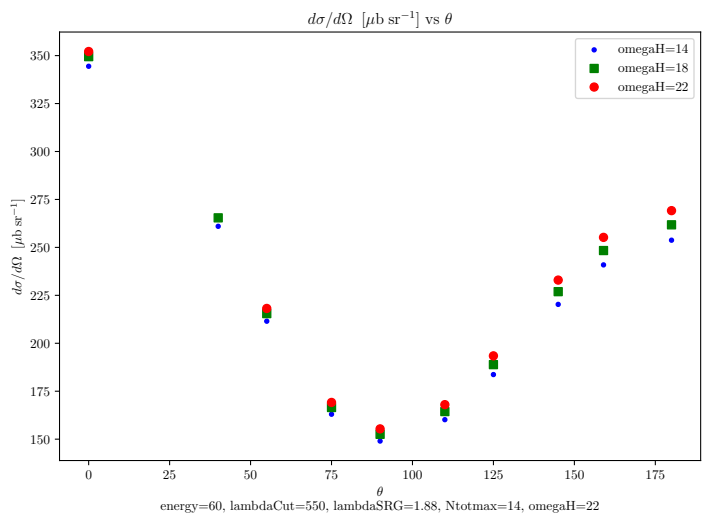

Figure 4: Caption

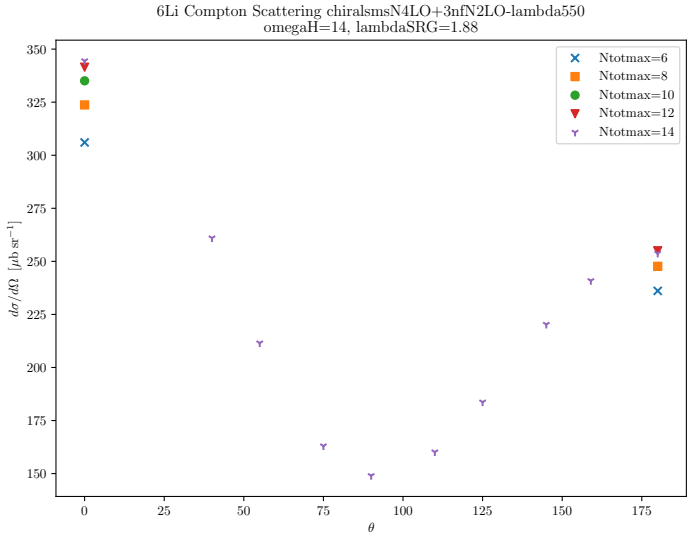

Figure 5: Caption

4. Analyzing Different Interactions

We are of course interested in Compton scattering but we also wish to extend the density formalism to other processes. In particular pion-photoproduction, and pion-pion scattering are of interest. Fortunately their kernels share remarkable similarity since there are a limited number of ways for one particle to go in and one to go out.

4.1 Compton Scattering

Compton scattering allows for extraction of the nucleon polarizabilites. Specifically, the nucelon electric and magnetic polarizabilities, α_{E1}, β_{M1}, are subjects of much experimental interest. These parameters quantify the stiffness of a nucleus, and enter in the Hamiltonian via

$$\mathcal{H} = -4\pi \left(\frac{1}{2}\alpha_{E1}\vec{E}^2 + \frac{1}{2}\beta_{M1}\vec{H}^2 \right) \tag{10}$$

There have been many experiments on ^{6}Li, yet to date there is no theory prediction [10, 11]. We seek to fill this gap.

4.2 Pion-Photoproduction

For the pion-photoproduction one-body kernel, we use the results from a single nucleon scattering, $\gamma N \to \pi N$ which has been studied extensively [5, 13–15]. Its differential cross section can be decomposed in terms of the electric and magnetic multipoles $E_{l\pm}, M_{l\pm}$ which are angle independent [5]. Over the years, many experimental results have measured these multipoles to high order and with good precision such as "Unified Chew-Mandelstam SAID analysis..." Workman *et al.*[6]. The resulting scattering matrices $\mathcal{M}$ are exactly what enters as $\hat{O}_3$ in equation (6). This approach solves a significant problem since the calculation of the one-body pion-photoproduction

kernel to high accuracy directly from Feynman diagrams requires including many terms in the chiral expansion due to the proximity of the $\Delta(1232)$ resonance at $\sim$ 200MeV [7].

The two-body contributions do not easily decompose into multipole interactions, therefore we perform the calculation through expansions in the chiral Lagrangian through calculation of Feynman diagrams. It is likely this will lead to large uncertainties, as in the one-body case. At threshold energy, this reaction kernel has been analyzed by Lenkewitz *et al.*[8, 9]. We now have a numerically stable result for ^{3}He and seek to extend this approach to new targets. *Include some numbers*

4.3 Pion-Pion scattering and other reactions

The pion-pion scattering kernel is similar in structure to the pion-photoproduction kernel. Beane *et al.*have developed the pion-pion kernel at threshold for both one-body and two-body interactions [12]. We may extend this analysis to finite energy *You have a note here I cannot make out, it looks like "cheis as well?".* Once the pion-photoproduction and pion-pion scattering kernels have successfully been developed, we will be able to calculate all of these reactions on previously analyzed targets in the density formalism since we already have produced the TDAs required. In particular, we will calculate all of these reactions with the targets ^{3}H, ^{3}He, ^{4}He, and ^{6}Li. *are we actually doing* ^{3}H*?*

5. Conclusion

References

[1] H. W. Grießhammer, J. A. McGovern, A. Nogga, and D. R. Phillips, "Scattering Observables from One- and Two-body Densities: Formalism and Application to γ^3 Scattering," *Few-Body Systems*, vol. 61, no. 4, Nov. 2020. DOI: 10.1007/s00601-020-01578-w.

[2] P. Reinert, H. Krebs, and E. Epelbaum, "Semilocal momentum-space regularized chiral two-nucleon potentials up to fifth order," *The European Physical Journal A*, vol. 54, no. 5, May 2018. DOI: 10.1140/epja/i2018-12516-4.

[3] H. W. Griesshammer, J. Liao, J. A. McGovern, A. Nogga, and D. R. Phillips, "Compton Scattering on 4He with Nuclear One- and Two-Body Densities," arXiv:2401.16995.

[4] S. Szpigel and R. J. Perry, "The Similarity Renormalization Group,". arXiv:hep-ph/0009071.

[5] R. L. Walker, "Phenomenological Analysis of Single-Pion Photoproduction," *Phys. Rev.*, vol. 182, no. 5, pp. 1729–1748, Jun. 1969. DOI: 10.1103/PhysRev.182.1729.

[6] R. L. Workman, M. W. Paris, W. J. Briscoe, and I. I. Strakovsky, "Unified Chew-Mandelstam SAID analysis of pion photoproduction data," *Phys. Rev. C*, vol. 86, no. 1, p. 015202, Jul. 2012. DOI: 10.1103/PhysRevC.86.015202.

[7] N. Rijneveen, A. M. Gasparyan, H. Krebs, and E. Epelbaum, "Pion photoproduction in chiral perturbation theory with explicit treatment of the $\Delta(1232)$ resonance," arXiv:2108.01619.

[8] M. Lenkewitz, E. Epelbaum, H.-W. Hammer, and U.-G. Meißner, "Neutral pion photoproduction off ^{3}H and ^{3}He in chiral perturbation theory," *Physics Letters B*, vol. 700, no. 5, pp. 365–368, Jun. 2011. DOI: 10.1016/j.physletb.2011.05.036.

[9] M. Lenkewitz, E. Epelbaum, H.-W. Hammer, and U.-G. Meissner, "Threshold neutral pion photoproduction off the tri-nucleon to $O(q^4)$," *The European Physical Journal A*, vol. 49, no. 2, Feb. 2013. DOI: 10.1140/epja/i2013-13020-1.

[10] L. S. Myers, M. W. Ahmed, G. Feldman, A. Kafkarkou, D. P. Kendellen, I. Mazumdar, J. M. Mueller, M. H. Sikora, H. R. Weller, and W. R. Zimmerman, "Compton scattering from ^{6}Li at 86 MeV," *Phys. Rev. C*, vol. 90, no. 2, p. 027603, Aug. 2014. DOI: 10.1103/PhysRevC.90.027603.

[11] L. S. Myers, M. W. Ahmed, G. Feldman, S. S. Henshaw, M. A. Kovash, J. M. Mueller, and H. R. Weller, "Compton scattering from ^{6}Li at 60 MeV," *Phys. Rev. C*, vol. 86, no. 4, p. 044614, Oct. 2012. DOI: 10.1103/PhysRevC.86.044614.

[12] S. R. Beane, V. Bernard, E. Epelbaum, U.-G. Meißner, and D. R. Phillips, "The S-wave pion–nucleon scattering lengths from pionic atoms using effective field theory," *Nuclear Physics A*, vol. 720, no. 3–4, pp. 399–415, Jun. 2003. DOI: 10.1016/S0375-9474(03)01008-X.

[13] N. Rijneveen, A. M. Gasparyan, H. Krebs, and E. Epelbaum, "Pion photoproduction in chiral perturbation theory with explicit treatment of the $\Delta(1232)$ resonance," 2021. Available: arXiv:2108.01619.

[14] R. L. Workman, M. W. Paris, W. J. Briscoe, and I. I. Strakovsky, "Unified Chew-Mandelstam SAID analysis of pion photoproduction data," *Phys. Rev. C*, vol. 86, no. 1, p. 015202, Jul. 2012. DOI: 10.1103/PhysRevC.86.015202.

[15] W. J. Briscoe, A. Schmidt, I. Strakovsky, R. L. Workman, and A. Švarc, "Extended SAID partial-wave analysis of pion photoproduction," *Phys. Rev. C*, vol. 108, no. 6, p. 065205, Dec. 2023. DOI: 10.1103/PhysRevC.108.065205.

[16] R. J. Furnstahl and K. Hebeler, "New applications of renormalization group methods in nuclear physics," *Reports on Progress in Physics*, vol. 76, no. 12, p. 126301, Nov. 2013. DOI: 10.1088/0034-4885/76/12/126301.

[17] X.-X. Sun, H. Le, A. Nogga, and U.-G. Meißner, in preparation (2025).